



## ORIGINAL ARTICLE

# MicroRNA-326 negatively regulates CD155 expression in lung adenocarcinoma

Takayuki Nakanishi<sup>1</sup> | Yasuto Yoneshima<sup>1</sup>  | Koji Okamura<sup>1</sup> | Toyoshi Yanagihara<sup>1</sup> | Mikiko Hashisako<sup>2</sup> | Takeshi Iwasaki<sup>2</sup> | Naoki Haratake<sup>3</sup> | Shun Mizusaki<sup>1</sup> | Keiichi Ota<sup>1</sup> | Eiji Iwama<sup>1</sup>  | Tomoyoshi Takenaka<sup>3</sup> | Kentaro Tanaka<sup>1</sup> | Tomoharu Yoshizumi<sup>3</sup> | Yoshinao Oda<sup>2</sup>  | Isamu Okamoto<sup>1</sup>

<sup>1</sup>Department of Respiratory Medicine, Graduate School of Medical Sciences, Kyushu University, Fukuoka, Japan

<sup>2</sup>Department of Anatomic Pathology, Graduate School of Medical Sciences, Kyushu University, Fukuoka, Japan

<sup>3</sup>Department of Surgery and Science, Graduate School of Medical Sciences, Kyushu University, Fukuoka, Japan

## Correspondence

Yasuto Yoneshima, Department of Respiratory Medicine, Graduate School of Medical Sciences, Kyushu University, 3-1-1 Maidashi, Higashi-ku, Fukuoka 812-8582, Japan.

Email: [yoneshima.yasuto.926@m.kyushu-u.ac.jp](mailto:yoneshima.yasuto.926@m.kyushu-u.ac.jp)

## Funding information

Japan Society for the Promotion of Science, Grant/Award Number: KAKENHI/21K15553

## Abstract

Treatment with immune checkpoint inhibitors induces a durable response in some patients with non-small-cell lung cancer, but eventually gives rise to drug resistance. Upregulation of CD155 expression is implicated as one mechanism of resistance to programmed death receptor-1 (PD-1)/PD-1 ligand (PD-L1) inhibitors, and it is therefore important to characterize the mechanisms underlying regulation of CD155 expression in tumor cells. The aim of this study was to identify microRNAs (miRNAs) that might regulate CD155 expression at the posttranscriptional level in lung cancer. Comprehensive miRNA screening with target prediction programs and a dual-luciferase reporter assay identified miR-346, miR-328-3p, miR-326, and miR-330-5p as miRNAs that bind to the 3'-UTR of *CD155* mRNA. Forced expression of these miRNAs suppressed CD155 expression in lung cancer cell lines. Immunohistochemical staining of CD155 in tissue specimens from 57 patients with lung adenocarcinoma revealed the median tumor proportion score for CD155 to be 68%. The abundance of miR-326 in these specimens with a low level of CD155 expression was significantly greater than in specimens with a high level ( $p < 0.005$ ). Our results thus suggest that miR-326 negatively regulates CD155 expression in lung adenocarcinoma and might therefore play a role in the development of resistance to PD-1/PD-L1 inhibitors.

## KEYWORDS

CD155, lung adenocarcinoma, microRNA, miR-326, nectin-like molecule 5 (Nect5), poliovirus receptor (PVR)

**Abbreviations:** E:T, effector:target; ICI, immune checkpoint inhibitor; IFN- $\gamma$ , interferon- $\gamma$ ; LDH, lactate dehydrogenase; LNA, locked nucleic acid; MFI, median fluorescence intensity; miR, microRNA; miRNA, microRNA; Nect5, nectin-like molecule 5; NSCLC, non-small-cell lung cancer; OD, optical density; PD-1, programmed death receptor-1; PD-L1, programmed cell death 1-ligand 1; PVR, poliovirus receptor; qPCR, quantitative PCR; TIGIT, T cell immunoreceptor with Ig and ITIM domains; TPS, tumor proportion score.

This is an open access article under the terms of the [Creative Commons Attribution-NonCommercial](https://creativecommons.org/licenses/by-nc/4.0/) License, which permits use, distribution and reproduction in any medium, provided the original work is properly cited and is not used for commercial purposes.

© 2023 The Authors. *Cancer Science* published by John Wiley & Sons Australia, Ltd on behalf of Japanese Cancer Association.

## 1 | INTRODUCTION

Cancer cells evade immune surveillance by expressing multiple immune checkpoint molecules.<sup>1</sup> Immune checkpoint inhibitors that target inhibitory signaling in T cells mediated by the interaction of PD-1 with its ligand (PD-L1) have shown unprecedented clinical activity for the treatment of NSCLC without targetable mutations of *EGFR* or *ALK* genes, having become a standard therapy for this disease.<sup>2–6</sup> Expression of PD-L1 in tumor cells has been found to be related to the response to PD-1/PD-L1 inhibitors and has been approved as a biomarker for such treatment in individuals with NSCLC. However, not all PD-L1-positive patients respond to these agents, with the identification of new drug resistance biomarkers and development of new therapies being clinical priorities.<sup>7,8</sup>

CD155, also known as PVR and Necl5, is often upregulated in tumor cells and endows them with a growth advantage and increased migratory capacity.<sup>9,10</sup> It also binds with high affinity to the immune checkpoint molecule TIGIT and thereby inhibits T cell activation,<sup>11</sup> and recent evidence suggests that it might mediate resistance to ICIs in melanoma and NSCLC.<sup>12–15</sup> A phase II study provided preliminary evidence for the efficacy and safety of combination therapy with Abs to TIGIT and to PD-L1 for advanced NSCLC,<sup>16</sup> with such therapy offering the potential to overcome resistance to PD-1/PD-L1 inhibitors. Multiple pathways could contribute to the expression and function of CD155 related to immune suppression, with a detailed understanding of the upregulation of CD155 in tumor cells having been lacking.

MicroRNAs are a class of small noncoding RNAs that comprise 19–25 nt and mediate posttranscriptional regulation of gene expression by binding to the 3'-UTR of protein-coding mRNAs with imperfect complementarity, with such binding resulting in inhibition of translation or in transcript cleavage.<sup>17</sup> Several miRNAs expressed in immune cells or cancer cells have been found to play key roles in cancer-related immune responses by targeting immunosuppressive or immunostimulatory factors.<sup>18</sup> Moreover, miRNAs regulate the expression of genes for immune checkpoint ligands such as PD-L1.<sup>19–21</sup>

Given the growing evidence implicating upregulation of CD155 in tumor cells in immune evasion, we have now investigated the possible role of miRNAs in the posttranscriptional regulation of CD155 expression in lung adenocarcinoma. Comprehensive miRNA screening with sequence-based target prediction algorithms and the use of a luciferase reporter assay allowed us to identify several miRNAs as potential regulators of CD155 expression in lung adenocarcinoma.

## 2 | MATERIALS AND METHODS

### 2.1 | MicroRNA target prediction

Seven target prediction programs—including TargetScan ([https://www.targetscan.org/vert\\_80](https://www.targetscan.org/vert_80)), miRMap (<http://mirmap.ezlab.org>), RNA22 (<https://cm.jefferson.edu/rna22>), miRWalk (<http://zmf.umm.uni-heidelberg.de>), miRanda ([www.microrna.org](http://www.microrna.org)), microT-CDS ([https://dianalab.e-ce.uth.gr/html/dianauniverse/index](https://dianalab.e-ce.uth.gr/html/dianauniverse/index.php?r=microT_CDS)),

<http://www.mirdb.org>)—were applied to screen for miRNAs that potentially bind to the 3'-UTR of CD155 mRNA.

### 2.2 | Cell culture and reagents

The human lung cancer cell lines A549, H322, and H23 as well as the human embryonic kidney cell line HEK293T were obtained from ATCC. Cells were cultured under 5% CO<sub>2</sub> at 37°C in DMEM for A439 and HEK293T cells and RPMI-1640 medium for H322 and H23 (Thermo Fisher Scientific), each supplemented with 10% FBS and 1% penicillin–streptomycin (Thermo Fisher Scientific).

Recombinant human IFN- $\gamma$  (Peprotech) was dissolved in PBS containing 0.1% BSA.

### 2.3 | MicroRNA transfection

Cells were transiently transfected during the exponential growth phase with 50 nM miScript miR-346 mimic (ID:MSY0000773), miScript miR-330-5p mimic (ID:MSY0004693), miScript miR-326 mimic (ID:MSY0000756), miScript miR-423-5p mimic (ID:MSY0004748), miRCURY LNA miR-328-3p mimic (ID:YM00473147), miRCURY LNA miR-6884-5p mimic (ID:YM00472866), miRCURY LNA miR-485-5p mimic (ID:YM00473278), miRCURY LNA miR-1306-5p mimic (ID:YM00473249), miRCURY LNA miR-423-5p mimic (ID:MSY0004748), miRCURY LNA miR-324-5p mimic (ID:YM00473205), mirVana miR-3184-5p mimic (ID:PM18582), or AllStars negative control (ID:SI03650318), all obtained from Qiagen. Transfection was carried out for 48 h with the use of the Lipofectamine RNAiMAX or Lipofectamine 3000 reagents (Thermo Fisher Scientific), and the cells were then subjected to experiments.

### 2.4 | Construction of CD155 overexpression plasmids

cDNA corresponding to the full-length 3'-UTR of CD155 mRNA was amplified by PCR from total cDNA of A549 cells with PrimeSTAR GXL DNA Polymerase (Takara) and the primers 5'-TAATTCTAGTTGTTTAACTAGCGGCCGCCAGCGTCGGGACTGAG-3' (forward) and 5'-GCATGCCTGCAGGTCGACTCTAGATTTTGCATTATTA AAGAAGAGTCAAGG-3' (reverse). Complementary 18–22 bp DNA oligonucleotides containing putative miR-346, miR-328-3p, miR-326, or miR-330-5p binding sites of the 3'-UTR of CD155 mRNA, or corresponding mutant sites, were synthesized. The sense and antisense strands were annealed by incubation of 2000 ng of each oligonucleotide in 46  $\mu$ L Oligo Annealing Buffer (Promega) first for 3 min at 90°C and then for 1 h at 37°C. The PCR amplicon for the full-length 3'-UTR of CD155 mRNA and the annealed oligonucleotides were separately cloned between the *PmeI* and *XbaI* sites of the pmirGLO Dual-Luciferase vector (Promega) with the

use of an In-Fusion HD Cloning Kit (Takara). The coding sequence of CD155 was amplified by PCR from total cDNA of A549 cells with PrimeSTAR GXL DNA Polymerase (Takara) and the primers 5'-GGACTCAGATCTCGAGGGAGCAACTGGCATGGC-3' (forward) and 5'-GTCGACTGCAGAATTCACGCTGTACCTTGTGC-3' (reverse). The PCR amplicon was cloned between the *Xho*I and *Eco*RI sites of the pIRES2-EGFP vector (BD Biosciences); the annealed oligonucleotides containing putative miRNA binding sites were cloned between the *Sall*I and *Sac*II sites. All plasmids used in this study were verified by Sanger sequencing.

## 2.5 | Luciferase reporter assay

Each reporter plasmid (100 ng) was introduced together with miRNA mimics (50 nM) or a negative control miRNA into HEK293T cells in 96-well plates by transfection for 48 h with the use of Lipofectamine 3000 reagents (Thermo Fisher Scientific). Luciferase activity in cell lysates was then measured with the use of a Dual-Luciferase Assay System (Promega), and firefly luciferase activity was normalized by *Renilla* luciferase activity.

## 2.6 | RNA extraction and RT-qPCR analysis

Total RNA was isolated from cultured cells with the use of an RNeasy Mini Kit or an miRNeasy Mini Kit (Qiagen). Total RNA from tissue samples was extracted with the use of an AllPrep DNA/RNA FFPE Kit (Qiagen). For analysis of the abundance of CD155 mRNA, total RNA (400 ng) was subjected to RT with PrimeScript RT Master Mix (Takara) and the resulting cDNA was subjected to qPCR analysis in triplicate with TB Green Premix Ex Taq II (Takara) in a Thermal Cycler Dice Real Time System (Takara). The qPCR primers (forward and reverse, respectively) were 5'-GGCAACTACAC CTGCCTGTT-3' and 5'-AATCACCTGGCACTCAGACC-3' for CD155 mRNA, 5'-AGCCAATAACCGAGAGAAGCG-3' and 5'-ATCTCACG GTTGCCACCTTC-3' for *ARRB1* mRNA and 5'-ACTCAACACGG GAAACCTCA-3' and 5'-AACCAGACAAATCGCTCCAC-3' for 18S rRNA (endogenous normalization control). For analysis of mature miRNAs, total RNA (10 ng) was subjected to RT with a miRCURY LNA RT Kit (Qiagen) and the resulting cDNA was subjected to qPCR analysis in triplicate with a miRCURY LNA SYBR Green PCR Kit (Qiagen) in a Thermal Cycler Dice Real Time System (Takara). The small nuclear RNAs U6 and SNORD38B were used as endogenous controls for lung cancer cell lines and tumor samples, respectively (Table S1). Relative mRNA or miRNA abundance was determined with SDS software (Applied Biosystems) by the  $2^{-\Delta\Delta Ct}$  method.

## 2.7 | Flow cytometry

For analysis of CD155 expression at the cell surface, cultured cells were harvested, suspended in ice-cold PBS supplemented with 1%

FBS, and incubated for 30 min on ice in the dark with phycoerythrin-conjugated mouse mAbs to human CD155 (diluted 1:100, #337610; BioLegend) or an IgG1  $\kappa$  isotype control (diluted 1:100, #400114; BioLegend). The cells were then subjected to flow cytometric analysis with a FACSVerse instrument (BD Biosciences) and Flowjo software (Tree Star). The relative MFI ratio was calculated as CD155 MFI divided by isotype-control MFI.

## 2.8 | Immunoblot analysis

Cultured cells were lysed in RIPA buffer (Thermo Fisher Scientific), the lysates were fractionated by SDS-PAGE, and the separated proteins were transferred to a PVDF membrane. The membrane was incubated overnight at 4°C with Abs to CD155 (diluted 1:1000, clone D8A5G, #81254; Cell Signaling Technology), and immune complexes were then detected with HRP-conjugated goat Abs to rabbit IgG (GE Healthcare), Pierce Western Blotting Substrate Plus (Thermo Fisher Scientific), and a ChemiDoc Touch MP system (Bio-Rad).  $\beta$ -Actin was detected with corresponding primary Abs (diluted 1:1000, clone 13E5, #4970; Cell Signaling Technology) and HRP-conjugated goat Abs to rabbit IgG (GE Healthcare) as a loading control.

## 2.9 | Patients and tissue samples

Formalin-fixed, paraffin-embedded tissue samples were collected retrospectively from 57 individuals who had undergone surgical resection of lung adenocarcinoma at Kyushu University Hospital between February and December 2020. Diagnosis of the 57 patients was based on the WHO Classification of Lung Tumors. All 57 samples were subjected to immunohistochemistry and RT-qPCR analysis. The characteristics of the patients were obtained from their medical records. This aspect of the study was carried out in accordance with the Declaration of Helsinki (as revised in 2013) and was approved by the Ethics Committee of Kyushu University and Kyushu University Hospital (ethics approval ID: 2021-289).

## 2.10 | Immunohistochemistry

All tumor samples were subjected to immunohistochemical analysis with rabbit mAbs to CD155 (clone D8A5G, #81254; Cell Signaling Technology) at a dilution of 1:200 and rabbit mAbs to PD-L1 (clone 28-8, #ab205921; Abcam) at a dilution of 1:400. Fixed sections were incubated with the primary Abs overnight at 4°C, after which immune complexes were detected with the use of a Histofine Simple Stain Max-PO Kit (Nichirei Biosciences) for CD155, an Envision FLEX + Linker (Agilent) for PD-L1, and the peroxidase substrate 3,3'-diaminobenzidine. All staining was evaluated by two investigators including a pathologist, and the TPS for CD155 and PD-L1 expression in tumor cells were determined as the percentage of viable

tumor cells showing staining at any intensity in a section containing at least 100 viable tumor cells.

## 2.11 | In situ hybridization

In situ hybridization was undertaken with an ISH Reagent Kit (Genostaff) following the manufacturer's instructions. Formalin-fixed paraffin-embedded tissue samples were sectioned at a thickness of 6 μm; the sections were deparaffinized with G-Nox (Genostaff, Tokyo, Japan), rehydrated through an ethanol series, and placed in PBS. The samples were fixed with 10% neutral buffered formalin (NBF) for 30 min at 37°C, washed in distilled water, placed in 0.2% HCl for 10 min at 37°C, washed in PBS, treated with 10 μg/mL proteinase K (Fujifilm) in PBS for 10 min at 37°C and washed in PBS. The sections were heat-treated in PBS for 10 min at 95°C, cooled immediately in PBS at room temperature, and placed in a coplin jar containing 1× G-Wash (Genostaff) equal to 1× SSC. The LNA probes were adjusted to 25 nM with G-Hybo-L (Genostaff), heat-treated for 15 min at 80°C, and cooled immediately on an ice block. Hybridization of the tissue sections with the probe was undertaken for 16 h at 40°C. The sections were then washed three times with 50% formamide in 2× G-Wash for 30 min at 40°C and five times in TBS-T (0.1% Tween-20 in TBS) at room temperature. After treatment with 1× G-Block (Genostaff) for 15 min at room temperature, the sections were incubated with anti-DIG AP conjugate (Roche) diluted 1:2000 with G-Block (diluted 1/50) in TBS-T for 1 h at room temperature. The sections were washed twice in TBS-T and then incubated in 100 mM NaCl, 50 mM MgCl<sub>2</sub>, 0.1% Tween-20, and 100 mM Tris-HCl at pH 9.5. Coloring reactions were carried out with NBT/BCIP Solution (Sigma-Aldrich) and then samples were washed in PBS. The sections were counterstained with Kernechtrot Stain Solution (Muto) and mounted with G-Mount (Genostaff) and Malinol (Muto). Probe IDs for hsa-miR-326 for Scramble-miR were YD00611660 and YD00699004 (Qiagen), respectively. Images were obtained as a Z-stack using an all-in-one fluorescence microscope (BZ-X800; Keyence) and Z-projection images were analyzed using BZ-X Analyzer software (BZ-H4A; Keyence).

## 2.12 | Coculture of cancer cells with preactivated PBMCs

Peripheral blood mononuclear cells were isolated from blood donated by healthy donors using BD Vacutainer Mononuclear Cell Preparation Tubes. The PBMCs were inoculated in 24-well plates (1.0 × 10<sup>6</sup> cells/well) in AIM-V medium (Thermo Fisher Scientific) (1 mL/well) supplemented with 10% heat-inactivated human male AB plasma (Sigma-Aldrich). Cells were stimulated with Dynabeads coated with anti-CD3 and anti-CD28 mAbs (Invitrogen) at a bead:cell ratio of 1:1. Recombinant human interleukin-2 (R&D Systems) at 100 IU/mL was added. The stimulation was carried out at 37°C and 5% CO<sub>2</sub>. Preactivated PBMCs were washed with

PBS, resuspended in fresh media and directly cocultured with A549 cells that had been transfected with miR-326 mimic or negative control 48 h prior at several E:T ratios. After 24 h of incubation, the amount of LDH in the supernatant of the coculture system was detected with the CytoTox96 nonradioactive assay (Promega) following the manufacturer's instructions. Cytotoxicity for each E:T ratio was calculated using a modified standard formula:  $(OD_{\text{experimental}} - OD_{\text{spontaneous targets}} - OD_{\text{spontaneous effectors}}) / (OD_{\text{maximum}} - OD_{\text{spontaneous targets}}) \times 100$ . This aspect of the study was carried out in accordance with the Declaration of Helsinki (as revised in 2013) and was approved by the Ethics Committee of Kyushu University and Kyushu University Hospital (ethics approval ID: 22343-00).

## 2.13 | Statistical analysis

Differences in miRNA abundance or luciferase reporter activity were assessed with Student's *t*-test or the Mann-Whitney *U*-test, as appropriate. All statistical analyses were undertaken with GraphPad Prism 8 (GraphPad Software). A *p* value of <0.05 was considered statistically significant.

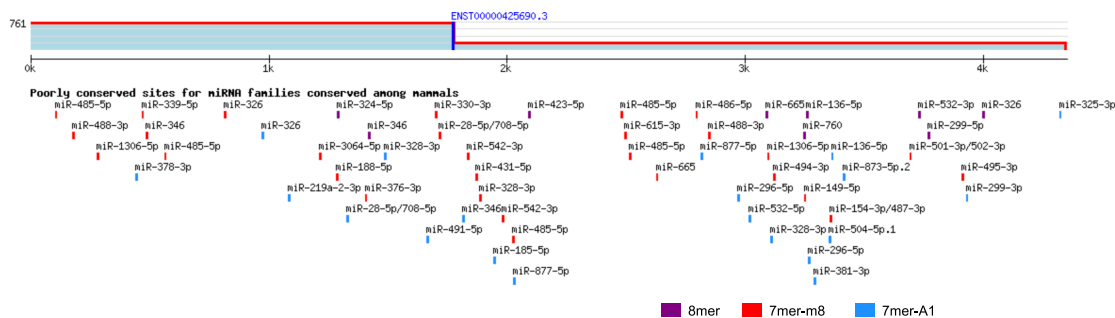
# 3 | RESULTS

## 3.1 | Identification of miRNAs as putative regulators of CD155 expression

To explore the possible regulation of CD155 expression by miRNAs, we identified miRNAs predicted to bind to the 3'-UTR of CD155 mRNA with the use of the TargetScan online prediction tool. A total of 48 miRNAs were predicted to bind to sites that are broadly conserved in the 3'-UTR of mammalian CD155 mRNA sequences (Figure 1A). We selected the 10 miRNAs with the highest TargetScan Total Context++ scores (Figure 1B) and tested them with a panel of six additional algorithms (miRMap, RNA22, miRWalk, miRanda, microT-CDS, and miRDB). All of the selected miRNAs were predicted to bind to the 3'-UTR of CD155 mRNA by at least three of these algorithms in addition to TargetScan (Figure 1C).

## 3.2 | Evaluation of miRNA binding to CD155 mRNA

To further evaluate miRNA binding to CD155 mRNA, we carried out a dual-luciferase reporter assay with the 10 predicted miRNAs. The coding sequence for the 4.3 kb full-length 3'-UTR of human CD155 mRNA was cloned downstream of the firefly luciferase gene in the pmirGLO Dual-Luciferase vector to yield pmirGLO-CD155 (Figure 2A), which was then introduced together with each miRNA mimic or a negative control miRNA into HEK293T cells by transfection. Six miRNAs (miR-346, miR-328-3p, miR-326, miR-330-5p, miR-6884-5p, and miR-324-5p) were found to attenuate normalized

**(A) Human PVR ENST00000425690.3 3' UTR length: 4350****(B)**

ID	Accession	TargetScan Total Context++ score
miR-346	MIMAT0000773	-0.62
miR-328-3p	MIMAT0000752	-0.49
miR-326	MIMAT0000756	-0.45
miR-330-5p	MIMAT0004693	-0.43
miR-6884-5p	MIMAT0027668	-0.35
miR-485-5p	MIMAT0002175	-0.33
miR-1306-5p	MIMAT0022726	-0.32
miR-423-5p	MIMAT0004748	-0.28
miR-324-5p	MIMAT0000761	-0.28
miR-3184-5p	MIMAT0015064	-0.26

**(C)**

ID	Accession	SUM	Target-Scan	miRMap	RNA22	miRWalk	miRanda	microT-CDS	miRDB
miR-346	MIMAT0000773	6	Orange	Orange	Orange	Orange	Orange	Orange	Orange
miR-328-3p	MIMAT0000752	4	Orange	Orange	Orange	Orange	Orange	Orange	Orange
miR-326	MIMAT0000756	6	Orange	Orange	Orange	Orange	Orange	Orange	Orange
miR-330-5p	MIMAT0004693	7	Orange	Orange	Orange	Orange	Orange	Orange	Orange
miR-6884-5p	MIMAT0027668	5	Orange	Orange	Orange	Orange	Orange	Orange	Orange
miR-485-5p	MIMAT0002175	4	Orange	Orange	Orange	Orange	Orange	Orange	Orange
miR-1306-5p	MIMAT0022726	5	Orange	Orange	Orange	Orange	Orange	Orange	Orange
miR-423-5p	MIMAT0004748	5	Orange	Orange	Orange	Orange	Orange	Orange	Orange
miR-324-5p	MIMAT0000761	5	Orange	Orange	Orange	Orange	Orange	Orange	Orange
miR-3184-5p	MIMAT0015064	5	Orange	Orange	Orange	Orange	Orange	Orange	Orange

**FIGURE 1** Identification of microRNAs (miRNAs) predicted to target *CD155* mRNA. (A) Location of predicted miRNA target sites in the 3'-UTR of human *CD155* mRNA (TargetScan version 8.0). Sites that are conserved among mammals are shown. (B) TargetScan Total Context++ scores of miRNAs predicted to bind to the 3'-UTR of *CD155* mRNA. (C) Results for screening the 10 miRNAs in (B) for binding to sites in the 3'-UTR of *CD155* mRNA with seven different sequence-based miRNA target prediction algorithms. Orange boxes indicate a positive result; SUM represents the number of algorithms yielding a positive result for each miRNA. PVR, poliovirus receptor.

firefly luciferase activity by at least 20% and were therefore determined to bind directly to the 3'-UTR of *CD155* mRNA (Figure 2B).

### 3.3 | Regulation of *CD155* expression by miRNAs in NSCLC cells

We next evaluated whether the six miRNAs found to bind to the 3'-UTR of *CD155* mRNA regulate *CD155* mRNA abundance in NSCLC cells. Transfection of A549 cells with these miRNA mimics (Figure S1) revealed that overexpression of miR-346, miR-328-3p, miR-326, and miR-330-5p each significantly reduced the abundance of *CD155* mRNA, whereas overexpression of miR-6884-5p or miR-324-5p had no such effect (Figure 3A). Overexpression of miR-346, miR-328-3p, miR-326, or miR-330-5p also significantly attenuated the expression of *CD155* at the cell surface as determined by flow cytometry (Figure 3B) as well as reduced the total abundance of *CD155* in cell lysates as determined by immunoblot analysis (Figure 3C). Similar inhibitory effects of these four miRNAs on cell surface expression of *CD155* were apparent in the NSCLC cell lines H322 and H23, with

the exception of miR-346 and miR-328-3p in H23 cells (Figure S2). These results thus indicated that miR-346, miR-328-3p, miR-326, and miR-330-5p regulate *CD155* expression in NSCLC cells.

### 3.4 | Validation of miRNA binding sites in the 3'-UTR of *CD155* mRNA

Our results indicated that miR-346, miR-328-3p, miR-326, and miR-330-5p bind directly to the 3'-UTR of *CD155* mRNA and suppress cell surface and total protein expression of *CD155* in NSCLC cells. TargetScan analysis predicted three binding sites for each of these miRNAs in the 3'-UTR of *CD155* mRNA. To confirm binding of each miRNA to these sites, we constructed dual-luciferase reporter plasmids containing each putative binding site with either the WT or a mutated sequence (Figure 4A-D). Transfection of HEK293T cells with these plasmids and the corresponding miRNA mimics revealed that each miRNA significantly inhibited the luciferase reporter activity for one of the three wild-type sequences, and that such inhibition was abolished by mutation of these sequences (Figure 4E-H).

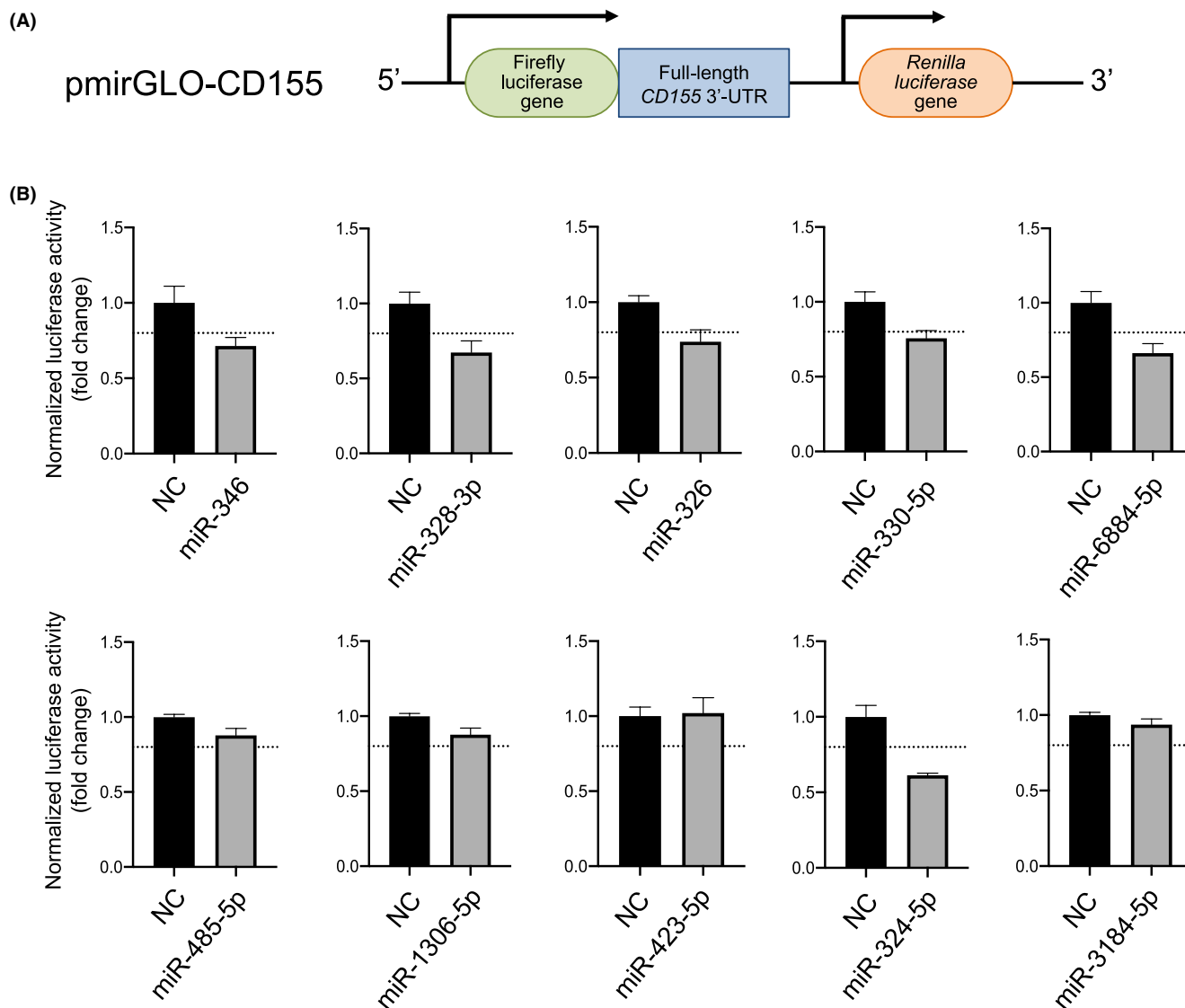


**FIGURE 2** Evaluation of microRNA (miRNA) binding to *CD155* mRNA with a luciferase reporter assay. (A) Schematic representation of the pmirGLO Dual-Luciferase vector containing the coding sequence for the full-length 3'-UTR of *CD155* mRNA (pmirGLO-*CD155*). (B) Luciferase reporter activity of HEK293T cells transfected with pmirGLO-*CD155* and the indicated miRNA mimics. Firefly luciferase activity was normalized by *Renilla* luciferase activity and then expressed as fold change relative to the normalized value for cells transfected with a negative control miRNA (NC). Data are means  $\pm$  SEM from three independent experiments. Those miRNAs that inhibited normalized luciferase activity by  $\geq 20\%$  were deemed to bind directly to the 3'-UTR of *CD155* mRNA.

These results indicated that miR-346, miR-328-3p, miR-326, and miR-330-5p each directly binds to at least one of the corresponding predicted sites in the 3'-UTR of *CD155* mRNA and thereby suppresses *CD155* expression.

### 3.5 | Association of miR-326 abundance and *CD155* expression in lung adenocarcinoma patients

To clarify further the role of miRNAs in the regulation of *CD155* expression in lung cancer, we determined the abundance of miR-346, miR-328-3p, miRNA-326, and miR-330-5p in *CD155*-low and *CD155*-high lung adenocarcinoma tissue. We collected tissue

specimens from 57 patients with lung adenocarcinoma who underwent surgical resection. The tissue was subjected to immunohistochemical staining of *CD155*, and the *CD155* TPS was determined (Figure 5A). The median TPS for *CD155* expression was 68% and was adopted as a cut-off for classification of the lung adenocarcinoma specimens as low or high for *CD155* expression. The clinical characteristics of the study patients according to *CD155* expression level are shown in Table 1. The proportions of men, former smokers, and tumors with higher pathological and TN stages tended to be greater for patients with *CD155*-high lung adenocarcinoma. The RT-qPCR analysis showed that the abundance of miR-326 was significantly lower in *CD155*-high tumors than in *CD155*-low tumors ( $p < 0.005$ ), whereas there was no

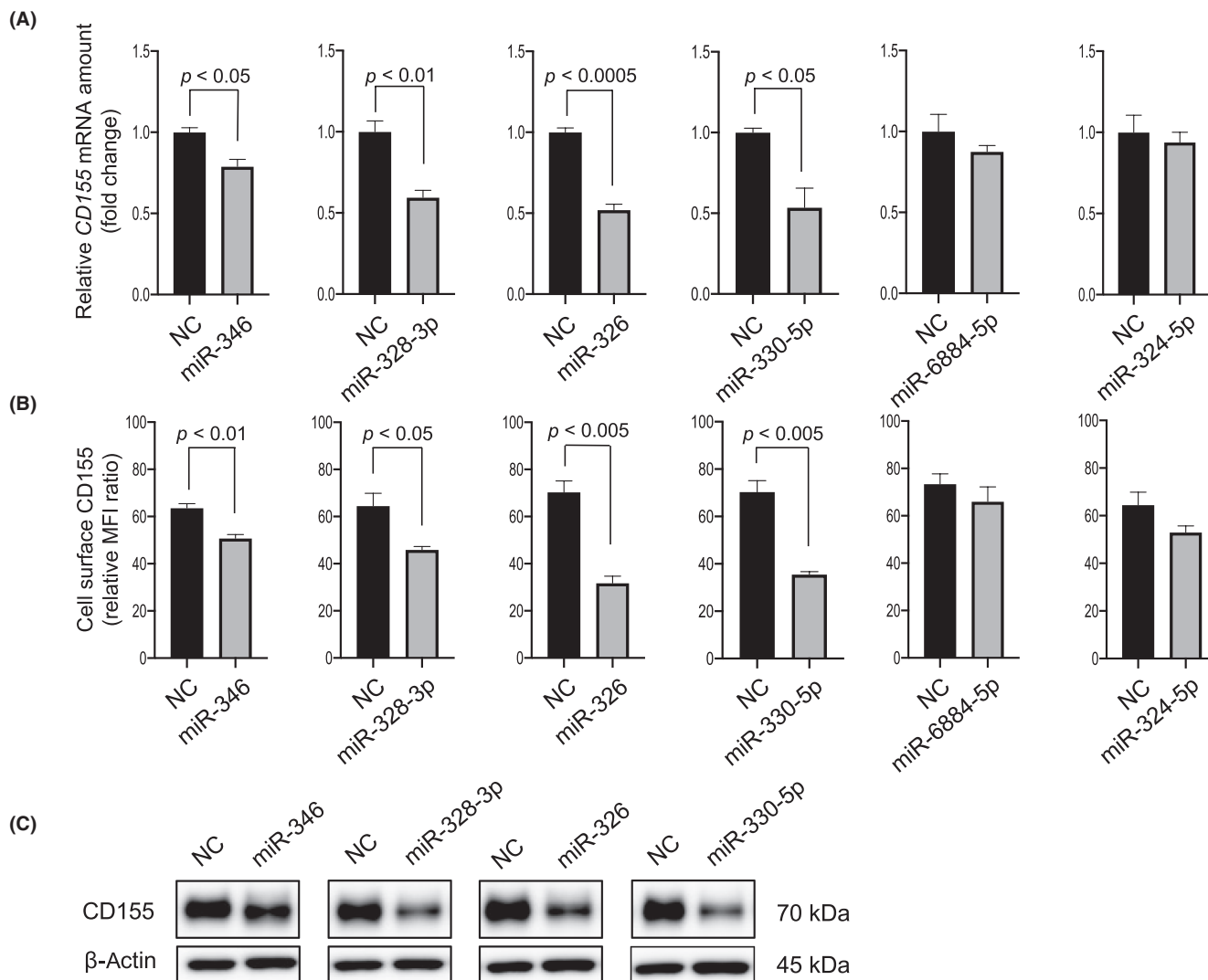


**FIGURE 3** Regulation of CD155 expression by microRNAs (miRNAs) in non-small-cell lung cancer cells. A549 cells transfected with miRNA mimics or a negative control miRNA (NC) were subjected to RT-qPCR analysis of CD155 mRNA abundance (A), to flow cytometric analysis of CD155 expression at the cell surface (B), and to immunoblot analysis of total CD155 abundance in cell lysates (C). Quantitative data are means  $\pm$  SEM from three independent experiments. Statistical analysis was undertaken with Student's *t*-test.

significant difference in the expression levels of miR-346, miR-328-3p, or miR-330-5p between CD155-low and CD155-high tumors (Figure 5B).

MicroRNAs are expressed in various type of cells, including tumor cells and the surrounding cells.<sup>22</sup> To determine the specific cells expressing miR-326 in the tumor microenvironment, we carried out in situ hybridization in lung adenocarcinoma tissues. MicroRNA-326 was detected in a variety of cells, including tumor cells, epithelial cells, and surrounding lymphocytes (Figure S3). The in situ hybridization results also showed that the signal intensity of miR-326 was lower in CD155-high tumors compared with CD155-low tumors. These results indicated that the abundance of miR-326 is negatively associated with CD155 expression in lung adenocarcinoma.

Recent studies reported that miR-326 repressed the gene expression of immune checkpoint ligands including PD-L1 in lung adenocarcinoma.<sup>23</sup> Tissue specimens from 57 patients were subjected

to immunohistochemical staining for PD-L1, and the PD-L1 TPS was determined (Figure S4A). We assessed the correlation between miR-326 and PD-L1 expression, and the results revealed significantly higher levels in the expression levels of miR-326 in PD-L1 <1% tumors compared with PD-L1  $\geq$ 1% tumors ( $p < 0.001$ ) (Figure S4B). These results confirmed that the abundance of miR-326 is also associated with PD-L1 expression in lung adenocarcinoma.

### 3.6 | Functional relevance of miR-326-induced CD155 downregulation in antitumor immune activity

Our results showed that overexpression of miR-326 led to suppression of CD155 expression in lung cancer cells and lung adenocarcinomas. To explore the regulatory factors governing miRNA-326 expression, we measured the expressions of *ARRB1*, the host gene

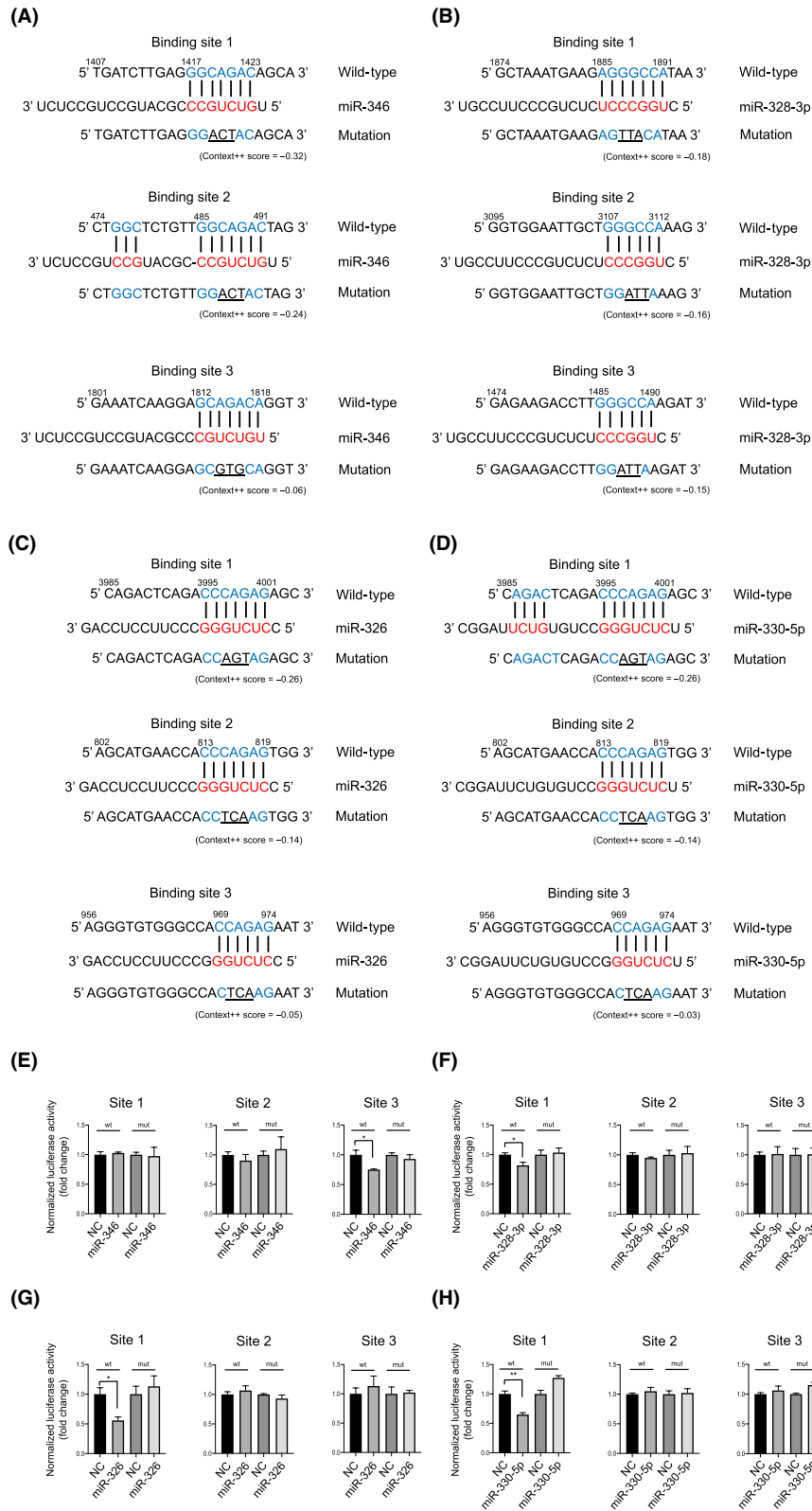


**FIGURE 4** Confirmation of microRNA (miRNA) binding sites in the 3'-UTR of *CD155* mRNA. (A–D) TargetScan analysis predicted three binding sites in the 3'-UTR of *CD155* mRNA for each of miR-346, miR-328-3p, miR-326, and miR-330-5p, and dual-luciferase reporter plasmids containing wild-type (wt) or mutant (mut) sequences for each of these putative binding sites were constructed. (E–H) Normalized luciferase reporter activity for HEK293T cells transfected with the luciferase reporter plasmids and either the corresponding miRNA mimic or a negative control miRNA (NC). Data are means + SEM from three independent experiments. \* $p < 0.05$ , \*\* $p < 0.005$  (Student's *t*-test).

of miR-326, and miR-326 in A549 cells treated with IFN- $\gamma$ , a major stimulator of antitumor immune responses.<sup>24</sup> Our results showed that IFN- $\gamma$  treatment significantly suppressed the expression of both *ARRB1* and miR-326 ( $p < 0.01$  and  $p < 0.05$ , respectively) (Figure 6A). These data indicate that the expression of miR-326 and *ARRB1* are regulated in response to IFN- $\gamma$  stimulation.

To determine whether downregulation of *CD155* by miR-326 would affect the antitumor immune activity, we undertook an LDH assay as described in a previous study.<sup>25</sup> A549 cells were transfected with miR-326 and then cocultured with activated T cells from PBMCs. Activated T cells were composed of approximately 50% CD8<sup>+</sup> T cells, which expressed TIGIT, the inhibitory receptor



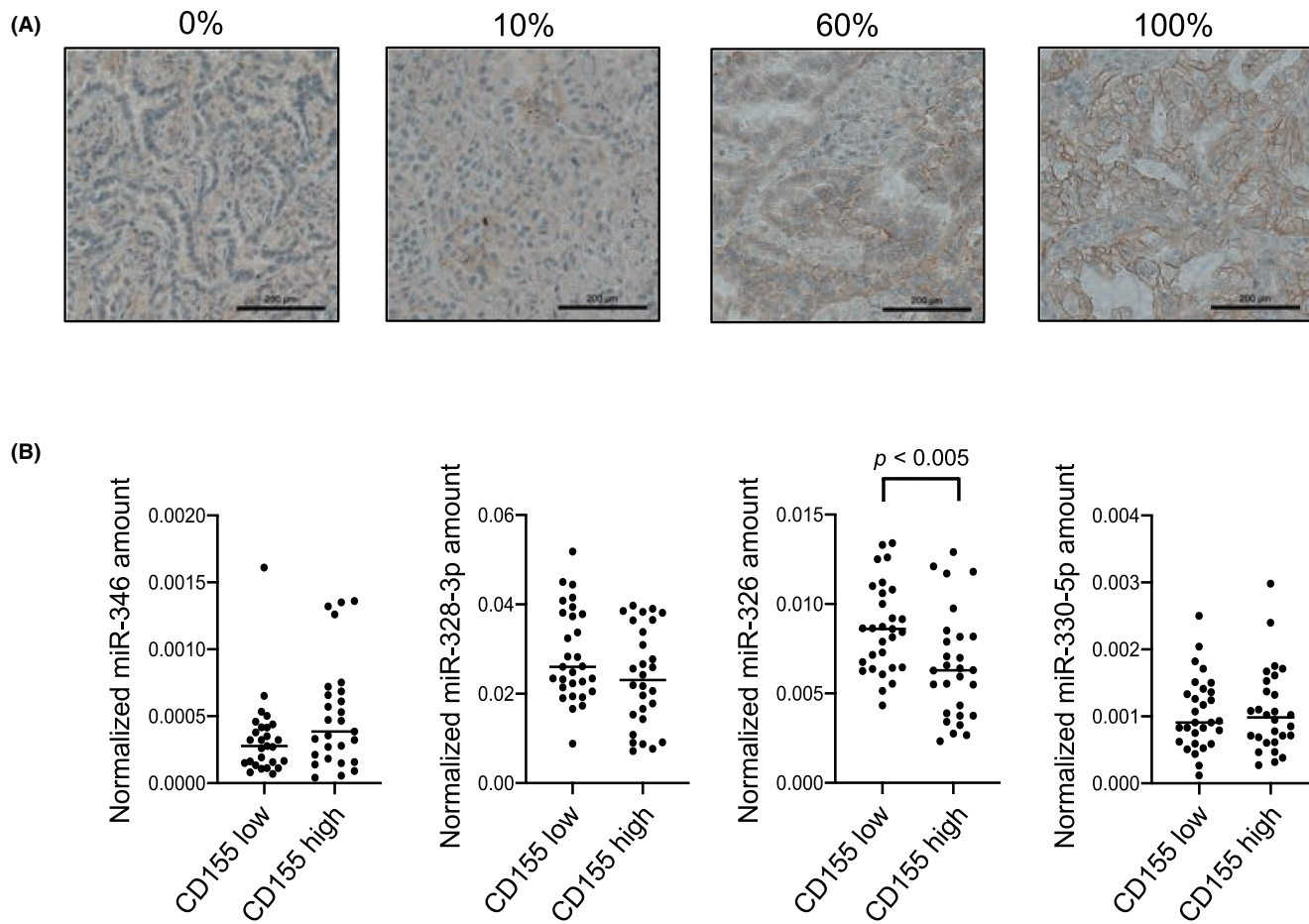


**FIGURE 5** Association of microRNA (miRNA) abundance and CD155 expression in lung adenocarcinoma. (A) Representative immunohistochemical staining of CD155 in lung adenocarcinoma specimens and the corresponding CD155 tumor proportion scores. Scale bar, 200 μm. (B) RT-qPCR analysis of miRNA abundance in lung adenocarcinoma specimens ( $n = 57$ ) according to CD155 expression level. Horizontal lines indicate median values. Statistical analysis was carried out with the Mann-Whitney  $U$ -test.

of CD155, as well as cytotoxic granules, perforin and granzyme B (Figure 6B). A significant increase in cell lysis was observed in A549 cells transfected with miR-326 compared with cells transfected with the negative control ( $p < 0.05$ ) (Figure 6C). These results indicate that suppression of CD155 enhanced the immune activity by activated T cells.

#### 4 | DISCUSSION

We set out to identify miRNAs that might regulate CD155 expression at the posttranscriptional level in lung cancer. We first applied target prediction algorithms and a luciferase reporter assay to discover functional miRNA binding sites in the 3'-UTR of CD155 mRNA. We then found that overexpression of four of the identified miRNAs (miR-346, miR-328-3p, miR-326, and miR-330-5p) suppressed CD155 expression as examined both at the cell surface and in cell lysates of lung cancer cell lines. Analysis of clinical samples revealed that miR-326 abundance was negatively associated with CD155 expression in patients with lung adenocarcinoma. Our

results have thus revealed a previously unrecognized mechanism for posttranscriptional regulation of CD155 expression in lung adenocarcinoma.

CD155 is a member (Nectin5) of the nectin-like molecule family and serves as the receptor for poliovirus (PVR).<sup>25</sup> Upregulation of CD155 has been detected in many cancer types including lung adenocarcinoma,<sup>15,26</sup> and its overexpression has been associated with tumor progression and poor prognosis in retrospective studies of various types of solid cancer.<sup>27</sup> In addition, CD155 overexpression promotes tumor cell invasion and migration as well as proliferation.<sup>28</sup> The upregulation of CD155 expression in tumors is likely due to a variety of mechanisms. Reactive oxygen species and reactive nitrogen species were shown to increase CD155 expression by inducing a DNA damage response in multiple myeloma cells.<sup>29</sup> Furthermore, IFN- $\gamma$  has been shown to increase CD155 expression in melanoma cells.<sup>30</sup> However, the mechanisms underlying regulation of CD155 expression in lung cancer have remained unclear.

We here identified miR-326 as an miRNA that negatively regulates CD155 expression in lung adenocarcinoma. Among four miRNAs found to regulate CD155 expression in lung cancer cells, forced

**TABLE 1** Baseline characteristics of study patients grouped in accordance with CD155 expression level

Characteristic	CD155 expression		Total
	Low (n=29)	High (n=28)	
Age (years)			
<70	15 (51.7)	14 (50.0)	29 (50.9)
≥70	14 (48.3)	14 (50.0)	28 (49.1)
Sex			
Male	12 (41.4)	16 (57.1)	28 (49.1)
Female	17 (58.6)	12 (42.9)	29 (50.9)
Smoking history			
Former smoker	14 (48.3)	19 (67.9)	33 (57.9)
Never smoker	15 (51.7)	9 (32.1)	24 (42.1)
Pathological stage			
Stage I	27 (93.1)	18 (64.3)	45 (78.9)
Stage II/III	2 (6.9)	10 (35.7)	12 (21.1)
T status			
T1	26 (89.7)	21 (75.0)	47 (82.5)
T2/T3/T4	3 (10.3)	7 (25.0)	10 (17.5)
N status			
N0	28 (96.6)	20 (71.4)	48 (84.2)
N1/N2/N3	1 (3.4)	8 (28.6)	9 (15.8)

Note: All values are number (%).

expression of miR-326 or miR-330-5p significantly suppressed CD155 expression in all three lung cancer cell lines examined (A549, H322, and H23). One possible reason why, among the four examined miRNAs, only miR-326 regulated CD155 expression in lung adenocarcinoma is that miR-326 might be more abundant than others in the tissue samples. However, further evaluation is needed to examine this issue.

Previous studies have found that miR-326 acts as a tumor suppressor in glioma and osteosarcoma.<sup>31-33</sup> A search of the miRBase database (<https://www.mirbase.org>) and TargetScan identified more than 300 potential target genes of miR-326, including that for *NSBP1* (nucleosome binding protein 1), which promotes cell proliferation and invasion and whose expression is suppressed by miR-326 in NSCLC cells.<sup>34</sup> Recent studies have also indicated that miR-326 directly binds to the mRNA for and suppresses the expression of *FSCN1* (fascin actin-bundling protein 1), which is implicated in the progression of lung cancer.<sup>35,36</sup> Notably, another study reported that miR-326 repressed the gene expression of immune checkpoint ligands including PD-L1 in lung adenocarcinoma.<sup>23</sup> These findings together with our results suggest that miR-326 might play an important role in the regulation of immune checkpoint ligands. In the present study, we now show that miR-326 directly binds to the mRNA for and suppresses the expression of CD155, which also contributes to tumor progression, consistent with the proposed role for miR-326 as a tumor suppressor.

Treatment with ICIs induces a durable response in some patients with NSCLC, but existing cancer immunotherapies are associated with both innate and acquired resistance.<sup>37,38</sup> Upregulation of CD155 is implicated as one mechanism of resistance to PD-1/PD-L1 inhibitors,<sup>14,15</sup> and it will therefore be important to identify the mechanisms underlying regulation of CD155 expression in tumors. However, repeated lung biopsy for the detection of resistance markers is highly invasive in patients with advanced lung cancer, with the development of biomarkers that can be measured with minimally invasive approaches being highly desirable. MicroRNAs detected in serum are thought to mediate intercellular communication by regulating gene expression at the posttranscriptional level in target cells.<sup>39-41</sup> Both intracellular and cell-free circulating miRNAs have been associated with the diagnosis and prognosis of lung cancer.<sup>42,43</sup> Our results now indicate that miR-326 in tumor cells or the tumor microenvironment suppresses CD155 expression in lung adenocarcinoma, suggesting that miR-326 present in serum might negatively regulate the expression of CD155 in lung cancer cells and that the serum level of miR-326 might be a resistance marker for PD-1/PD-L1 inhibitor treatment. MicroRNA-based therapeutics are currently being evaluated in clinical trials as new approaches for the treatment of malignancies and other diseases.<sup>44,45</sup> Because miR-326 acts as a tumor suppressor and activates T cells by inhibiting CD155 and PD-L1, miR-326 replacement could be useful as an immunotherapy for lung adenocarcinoma.

There are several limitations to the present study. First, the clinical samples were obtained from a relatively small patient population and at early disease stages, given that patients at an inoperable stage could not be included. Second, the clinical samples were limited to tumor tissue, with no corresponding serum samples being available. Third, the study explored miRNA-mediated regulation of CD155 expression largely in lung adenocarcinoma, with further investigation being necessary to assess the potential role of miR-326 in tumor or serum samples as a resistance biomarker for PD-1/PD-L1 inhibitors in patients with various cancer types. In addition to evaluation with the LDH assay, tumor antigen-specific experiments are also required to assess the precise function of CD155 in antitumor immunity.

In conclusion, our study has shown that miR-326 negatively regulates CD155 expression in lung adenocarcinoma. Our findings suggest that downregulation of miR-326 results in upregulation of CD155 expression and might therefore promote tumor progression and the development of resistance to PD-1/PD-L1 inhibitors.

#### AUTHOR CONTRIBUTIONS

Takayuki Nakanishi: Methodology, formal analysis, data curation, investigation, writing—original draft. Yasuto Yoneshima: Conceptualization, methodology, formal analysis, data curation, investigation, funding acquisition, project administration, writing—original draft, writing—review and editing. Koji Okamura: Methodology, writing—review and editing. Toyoshi Yanagihara: Methodology, writing—review and editing. Mikiko Hashisako: Methodology, writing—review and editing. Takeshi Iwasaki: Methodology, writing—review and editing. Naoki Haratake: Resources,

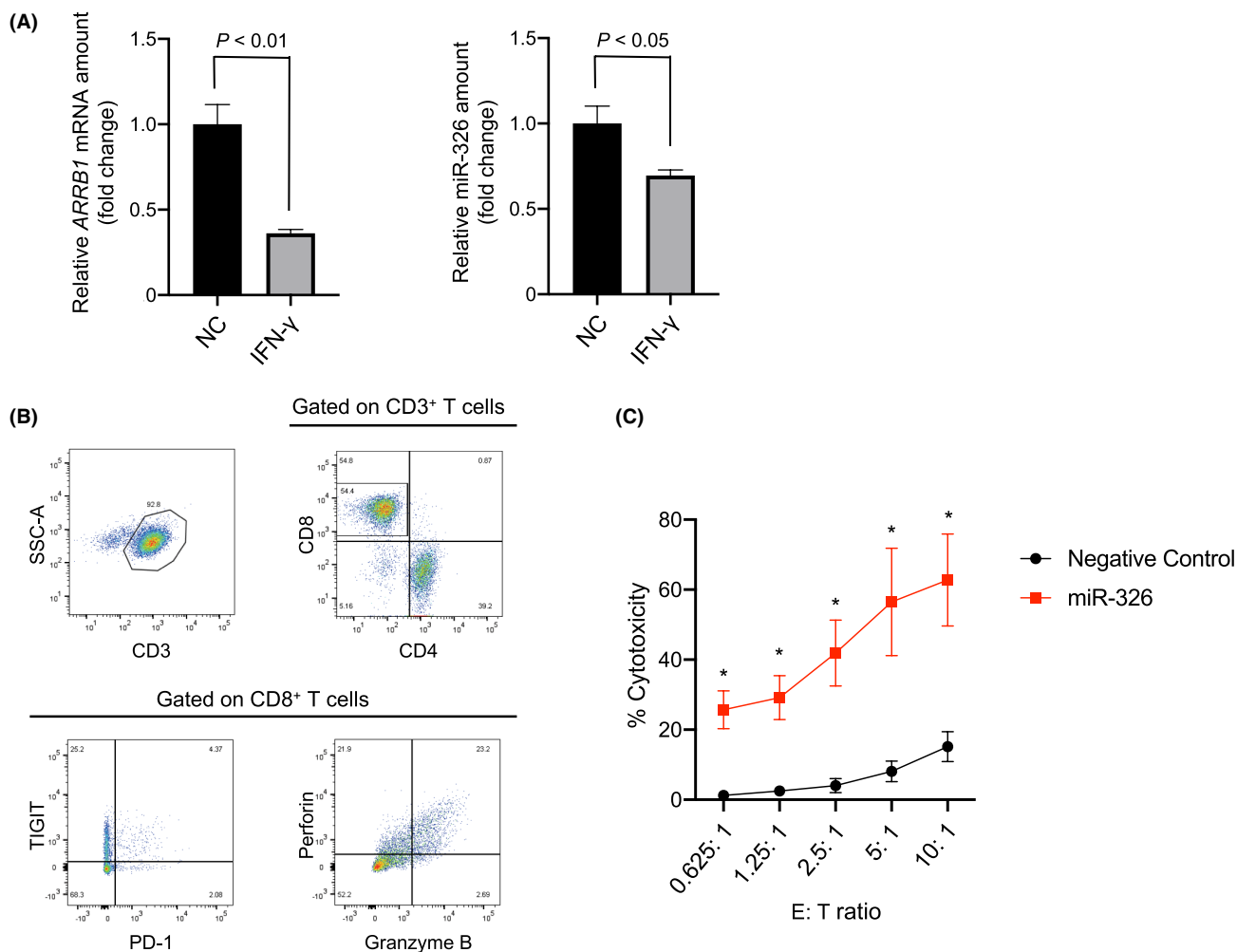


**FIGURE 6** Functional relevance of microRNA (miR)-326-induced CD155 downregulation in antitumor immune activity. (A) RT-qPCR analysis of the abundance of ARRB1, the host gene of miR-326, and miR-326 in A549 cells under treatment of 100  $\mu$ g/mL  $\gamma$ -interferon (IFN- $\gamma$ ). Data are means + SEM from three independent experiments. (B) Flow cytometric analysis of CD3, CD4/CD8, T cell immunoreceptor with Ig and ITIM domains (TIGIT)/programmed death receptor-1 (PD-1), and perforin/granzyme B at the cell surface for activated PBMCs with Dynabeads coated with anti-CD3 and anti-CD28 mAbs. (C) Lactate dehydrogenase assay in A549 cells transfected with miR-326 mimic or a negative control miRNA (NC) cocultured with activated T cells from PBMCs. E, effector cell (PBMC); T, target cell (A549). Data are means + SEM from three independent experiments. \* $p < 0.05$  (Student's *t*-test).

writing–review and editing. Shun Mizusaki: Methodology, writing–review and editing. Keiichi Ota: Methodology, writing–review and editing. Eiji Iwama: Methodology, writing–review and editing. Tomoyoshi Takenaka: Resources, writing–review and editing. Kentaro Tanaka: Methodology, writing–review and editing. Tomoharu Yoshizumi: Writing–review and editing. Yoshinao Oda: Writing–review and editing. Isamu Okamoto: Supervision, writing–review and editing.

#### ACKNOWLEDGMENTS

We thank Cell Innovator Co. Ltd. and The Research Support Center, Research Center for Human Disease Modeling, Kyushu University Graduate School of Medical Sciences, for technical assistance.

#### FUNDING INFORMATION

This work was supported by Japan Society for the Promotion of Science KAKENHI grant number 21K15553.

#### CONFLICT OF INTEREST STATEMENT

Y. Oda is an Editorial Board Member of *Cancer Science*. The other authors have no conflicts of interest to declare.

#### DATA AVAILABILITY STATEMENT

The data that support the findings of this study are available from the corresponding author, YY, upon reasonable request.

#### ETHICS STATEMENT

Approval of the research protocol by an institutional review board: The study was approved by the Ethics Committee of Kyushu University and Kyushu University Hospital (ethics approval ID: 2021-289, 22,343-00).

Informed consent: Informed consent was obtained from all healthy donors.

Registry and the registration no. of the study/trial: N/A.

Animal studies: N/A.

## ORCID

Yasuto Yoneshima  <https://orcid.org/0000-0002-0053-7241>Eiji Iwama  <https://orcid.org/0000-0001-8252-290X>Yoshinao Oda  <https://orcid.org/0000-0001-9636-1182>

## REFERENCES

1. Beatty GL, Gladney WL. Immune escape mechanisms as a guide for cancer immunotherapy. *Clin Cancer Res*. 2015;21:687-692.
2. Reck M, Rodríguez-Abreu D, Robinson AG, et al. Pembrolizumab versus chemotherapy for PD-L1-positive non-small-cell lung cancer. *N Engl J Med*. 2016;375:1823-1833.
3. Gandhi L, Rodríguez-Abreu D, Gadgeel S, et al. Pembrolizumab plus chemotherapy in metastatic non-small-cell lung cancer. *N Engl J Med*. 2018;378:2078-2092.
4. Paz-Ares L, Luft A, Vicente D, et al. Pembrolizumab plus chemotherapy for squamous non-small-cell lung cancer. *N Engl J Med*. 2018;379:2040-2051.
5. Hellmann MD, Paz-Ares L, Bernabe Caro R, et al. Nivolumab plus ipilimumab in advanced non-small-cell lung cancer. *N Engl J Med*. 2019;381:2020-2031.
6. Herbst RS, Giaccone G, de Marinis F, et al. Atezolizumab for first-line treatment of PD-L1-selected patients with NSCLC. *N Engl J Med*. 2020;383:1328-1339.
7. Sharma P, Hu-Lieskovan S, Wargo JA, Ribas A. Primary, adaptive, and acquired resistance to cancer immunotherapy. *Cell*. 2017;168:707-723.
8. Kawakami Y, Ohta S, Sayem MA, Tsukamoto N, Yaguchi T. Immune-resistant mechanisms in cancer immunotherapy. *Int J Clin Oncol*. 2020;25:810-817.
9. Masson D, Jarry A, Baury B, et al. Overexpression of the CD155 gene in human colorectal carcinoma. *Gut*. 2001;49:236-240.
10. Sloan KE, Eustace BK, Stewart JK, et al. CD155/PVR plays a key role in cell motility during tumor cell invasion and migration. *BMC Cancer*. 2004;4:73.
11. Manieri NA, Chiang EY, Grogan JL. TIGIT: a key inhibitor of the cancer immunity cycle. *Trends Immunol*. 2017;38:20-28.
12. Lepletier A, Madore J, O'Donnell JS, et al. Tumor CD155 expression is associated with resistance to anti-PD1 immunotherapy in metastatic melanoma. *Clin Cancer Res*. 2020;26:3671-3681.
13. Kawashima S, Inozume T, Kawazu M, et al. TIGIT/CD155 axis mediates resistance to immunotherapy in patients with melanoma with the inflamed tumor microenvironment. *J Immunother Cancer*. 2021;9:e003134.
14. Lee BR, Chae S, Moon J, et al. Combination of PD-L1 and PVR determines sensitivity to PD-1 blockade. *JCI Insight*. 2020;5:e128633.
15. Lee JB, Hong MH, Park SY, et al. Overexpression of PVR and PD-L1 and its association with prognosis in surgically resected squamous cell lung carcinoma. *Sci Rep*. 2021;11:8551.
16. Cho BC, Abreu DR, Hussein M, et al. Tiragolumab plus atezolizumab versus placebo plus atezolizumab as a first-line treatment for PD-L1-selected non-small-cell lung cancer (CITYSCAPE): primary and follow-up analyses of a randomised, double-blind, phase 2 study. *Lancet Oncol*. 2022;23:781-792.
17. Berindan-Neagoe I, Monroig Pdel C, Pasculli B, Calin GA. MicroRNAome genome: a treasure for cancer diagnosis and therapy. *CA Cancer J Clin*. 2014;64:311-336.
18. Paladini L, Fabris L, Bottai G, Raschioni C, Calin GA, Santarpia L. Targeting microRNAs as key modulators of tumor immune response. *J Exp Clin Cancer Res*. 2016;35:103.
19. Chen J, Jiang CC, Jin L, Zhang XD. Regulation of PD-L1: a novel role of pro-survival signalling in cancer. *Ann Oncol*. 2016;27:409-416.
20. Xie WB, Liang LH, Wu KG, et al. MiR-140 expression regulates cell proliferation and targets PD-L1 in NSCLC. *Cell Physiol Biochem*. 2018;46:654-663.
21. Ashizawa M, Okayama H, Ishigame T, et al. miRNA-148a-3p regulates immunosuppression in DNA mismatch repair-deficient colorectal cancer by targeting PD-L1. *Mol Cancer Res*. 2019;17:1403-1413.
22. Suzuki HI, Katsura A, Matsuyama H, Miyazono K. MicroRNA regulators in tumor microenvironment. *Oncogene*. 2015;34:3085-3094.
23. Shao L, He Q, Wang J, et al. MicroRNA-326 attenuates immune escape and prevents metastasis in lung adenocarcinoma by targeting PD-L1 and B7-H3. *Cell Death Dis*. 2021;7:145.
24. Chen DS, Mellman I. Oncology meets immunology: the cancer-immunity cycle. *Immunity*. 2013;39:1-10.
25. Gao J, Zheng Q, Xin N, Wang W, Zhao C. CD155, an onco-immunologic molecule in human tumors. *Cancer Sci*. 2017;108:1934-1938.
26. Nakai R, Maniwa Y, Tanaka Y, et al. Overexpression of Necl-5 correlates with unfavorable prognosis in patients with lung adenocarcinoma. *Cancer Sci*. 2010;101:1326-1330.
27. O'Donnell JS, Madore J, Li XY, Smyth MJ. Tumor intrinsic and extrinsic immune functions of CD155. *Semin Cancer Biol*. 2020;65:189-196.
28. Kakunaga S, Ikeda W, Shingai T, et al. Enhancement of serum- and platelet-derived growth factor-induced cell proliferation by Necl-5/Tag4/poliiovirus receptor/CD155 through the Ras-Raf-MEK-ERK signaling. *J Biol Chem*. 2004;279:36419-36425.
29. Fionda C, Abruzzese MP, Zingoni A, et al. Nitric oxide donors increase PVR/CD155 DNAM-1 ligand expression in multiple myeloma cells: role of DNA damage response activation. *BMC Cancer*. 2015;15:17.
30. Inozume T, Yaguchi T, Furuta J, Harada K, Kawakami Y, Shimada S. Melanoma cells control Antimelanoma CTL responses via interaction between TIGIT and CD155 in the effector phase. *J Invest Dermatol*. 2016;136:255-263.
31. Zhou J, Xu T, Yan Y, et al. MicroRNA-326 functions as a tumor suppressor in glioma by targeting the Nin one binding protein (NOB1). *PLoS One*. 2013;8:e68469.
32. Cao L, Wang J, Wang PQ. MiR-326 is a diagnostic biomarker and regulates cell survival and apoptosis by targeting Bcl-2 in osteosarcoma. *Biomed Pharmacother*. 2016;84:828-835.
33. Wang J, Cao L, Wu J, Wang Q. Long non-coding RNA SNHG1 regulates NOB1 expression by sponging miR-326 and promotes tumorigenesis in osteosarcoma. *Int J Oncol*. 2018;52:77-88.
34. Li D, Du X, Liu A, Li P. Suppression of nucleosome-binding protein 1 by miR-326 impedes cell proliferation and invasion in non-small cell lung cancer cells. *Oncol Rep*. 2016;35:1117-1124.
35. Luo A, Yin Y, Li X, Xu H, Mei Q, Feng D. The clinical significance of FSCN1 in non-small cell lung cancer. *Biomed Pharmacother*. 2015;73:75-79.
36. Zhang N, Nan A, Chen L, et al. Circular RNA circSATB2 promotes progression of non-small cell lung cancer cells. *Mol Cancer*. 2020;19:101.
37. Restifo NP, Smyth MJ, Snyder A. Acquired resistance to immunotherapy and future challenges. *Nat Rev Cancer*. 2016;16:121-126.
38. Wei SC, Duffy CR, Allison JP. Fundamental mechanisms of immune checkpoint blockade therapy. *Cancer Discov*. 2018;8:1069-1086.
39. Kosaka N, Iguchi H, Yoshioka Y, Takeshita F, Matsuki Y, Ochiya T. Secretory mechanisms and intercellular transfer of microRNAs in living cells. *J Biol Chem*. 2010;285:17442-17452.
40. Pegtel DM, Cosmopoulos K, Thorley-Lawson DA, et al. Functional delivery of viral miRNAs via exosomes. *Proc Natl Acad Sci U S A*. 2010;107:6328-6333.
41. Nishida-Aoki N, Ochiya T. Interactions between cancer cells and normal cells via miRNAs in extracellular vesicles. *Cell Mol Life Sci*. 2015;72:1849-1861.
42. Fehlmann T, Kahraman M, Ludwig N, et al. Evaluating the use of circulating MicroRNA profiles for lung cancer detection in symptomatic patients. *JAMA Oncol*. 2020;6:714-723.

43. Zhou Q, Huang SX, Zhang F, et al. MicroRNAs: a novel potential biomarker for diagnosis and therapy in patients with non-small cell lung cancer. *Cell Prolif*. 2017;50:e12394.
44. Rupaimoole R, Slack FJ. MicroRNA therapeutics: towards a new era for the management of cancer and other diseases. *Nat Rev Drug Discov*. 2017;16:203-222.
45. Ho PTB, Clark IM, Le LTT. MicroRNA-based diagnosis and therapy. *Int J Mol Sci*. 2022;23:7167.

**How to cite this article:** Nakanishi T, Yoneshima Y, Okamura K, et al. MicroRNA-326 negatively regulates CD155 expression in lung adenocarcinoma. *Cancer Sci*. 2023;114:4101-4113. doi:[10.1111/cas.15921](https://doi.org/10.1111/cas.15921)

#### SUPPORTING INFORMATION

Additional supporting information can be found online in the Supporting Information section at the end of this article.